

HOW DOES THE SIZE DISTRIBUTION OF LIVING MATERIAL INFLUENCE SOUND SCATTERING IN THE SEA?

JOANNA SZCZUCKA

Institute of Oceanology, Polish Academy of Sciences,
ul. Powstańców Warszawy 55, 81-712 Sopot, Poland,
szczucka@iopan.gda.pl

Evaluation of the relative contribution of the living objects with different sizes to sound scattering at sea is presented. The relative contribution to the total scattering depends on two factors: size spectrum of oceanic biomass and individual scattering properties of organisms. Various coefficients in the power function describing dependence of biomass concentration on individual size are tested and compared. Simple "high-pass" model of scattering is used. Flesh and swimbladder contributions are considered separately.

INTRODUCTION

A general formula for the distribution of the entire oceanic biomass, valid for all species from bacteria to whales, has been suggested in 1972 by Sheldon, Prakash and Sutcliffe [6]. This principle reveals roughly equal mass concentrations in logarithmically equal size categories. According to an ambiguous explanation of the abscissa, which is a particle diameter in Fig.2 of the above mentioned paper [6] and an individual particle volume in the text, this result becomes a source of two different size spectra formulations [3, 4].

If we assume that biomass is roughly equal in logarithmically equal volume intervals, then

$$\int_{V_1}^{2V_1} N(V)VdV = \int_{2V_1}^{4V_1} N(V)VdV . \quad (1a)$$

Integration leads to the expression

$$N(V) = C_1 V^{-2} \quad \Rightarrow \quad N(a) = B_1 a^{-6} . \quad (1b)$$

Alternatively understood concept of "flat biomass spectrum" assuming that mass concentration is approximately equal in logarithmically equal radius categories

$$\int_{a_1}^{2a_1} N(a) \mathcal{V} da = \int_{2a_1}^{4a_1} N(a) \mathcal{V} da \quad (2a)$$

gives

$$\int_{a_1}^{2a_1} N(a) a^3 da = \int_{2a_1}^{4a_1} N(a) a^3 da \Rightarrow N(a) = B_2 a^{-4}. \quad (2b)$$

In each case, concentration of the oceanic living matter is described by a power function:

$$N(a) = B a^{-\kappa}. \quad (3)$$

Since animals in the sea will be the major source of the backscattered sound waves, the interesting question arises: what is the influence of the shape of the function $N(a)$ on the sound scattering efficiency and which types of marine organisms are responsible for the scattering of acoustic waves at specified frequencies. To solve this problem one has to integrate the expression for the total backscattering cross-section of the unit volume in the limit from the minimum size till some specified size and compare it with the analogous integral embracing the entire radius interval $[a_{min}, a_{max}]$. The coefficient of volume backscattering (the total backscattering cross-section per unit volume) is defined in the following way:

$$S_V = \int_0^{a_{max}} N(a) \sigma_{bs}(a) da. \quad (4)$$

In order to evaluate S_V , the function describing biomass spectrum and appropriate model of scattering should be used. Integral function is a product of a monotonically decreasing function $N(a)$ and increasing $\sigma_{bs}(a)$, so our interest will focus on the trend of function $N \cdot \sigma_{bs}$. We expect the decreasing character of this product, in that case only the process of integration will converge.

1. SCATTERING MODELS

There exist various mathematical models describing the target strength of organisms with different degrees of complexity. There are different mechanisms of scattering for different types of zooplankton [e.g. 1, 2, 5, 7, 8]. Generally, there are two parallel ways of modelling based on the linearity principle:

- scattering models for single (individual) objects, often based on fitting the mathematical description to the experimental results
- scattering models for mixtures of organisms with different sizes, shapes, elastic parameters and spatial orientations.

Models of the first kind have an evident modal, oscillating structure. The effect of measurement of target strength of the individual object TS is characterised by large fluctuations between consecutive transmissions resulting from the animal movement and change in its tilt angle. In order to determine the mean value of TS we average the results of many realisations and then the modal structure disappears. Similarly, when we are measuring the mixture of various species, sizes and orientations, the modal structure is invisible.

For our purpose, we have chosen the so-called “high-pass” model of TS , originally introduced by Johnson [5] to describe sound scattering on the fluid sphere, and developed by Stanton [7] to describe scattering on the sphere, prolate spheroid, straight and bent cylinders, made of any materials: fluid, gas, elastic or rigid. For elongated bodies the Stanton’s model is valid for broadside incidence. Both models are quite sufficient to calculate the intensity of

sound backscattered on the aggregations of different type and different size of animals. The sphere model is the simplest of them, but ellipsoid and cylinder models additionally take into account the elongated shape and spatial orientation of the scatterer. According to Stanton [7] backscattering cross-section σ_{bs} of any object can be written as:

$$\sigma_{bs} = \frac{X}{1 + \frac{X}{YR^2}} = \frac{XY}{R^2 + Y} = \frac{Y}{\frac{1}{R^2} + \frac{Y}{X}}, \quad (5)$$

where X and Y are the exact expressions for σ_{bs} valid in specified object size – sound frequency regions of scattering (ka domains):

$$X = \sigma_{bs}(ka \ll 1, \text{fluid}),$$

$$Y = \sigma_{bs}(ka \gg 1, \text{rigid/fixed}).$$

Expressions for X and Y for different shapes of scatterers are shown in Table 1.

Table 1. Backscattering cross-sections for $ka \ll 1$ and $ka \gg 1$ for different shapes of scatterers.

	X	Y
sphere	$a^2 (ka)^4 \alpha_{\pi s}^2$	$\frac{1}{4} a^2$
ellipsoid	$\frac{1}{9} L^2 (ka)^4 \alpha_{\pi c}^2$	$\frac{1}{16} L^2$
bent cylinder	$\frac{1}{4} L^2 (ka)^4 \alpha_{\pi c}^2 H^2$	$\frac{1}{4} \rho_c a$

where:

a – radius of sphere or semi-minor axis of ellipsoid or radius of cylinder,

L – ellipsoid major axis or cylinder length,

k – wave number,

ρ_c – radius of curvature of bent cylinder,

$$H = \frac{1}{2} + \frac{1}{2} \frac{\rho_c}{L} \sin\left(\frac{L}{\rho_c}\right), \quad (6)$$

$$R = \frac{1 - gh}{1 + gh} \quad \text{– Rayleigh reflection coefficient}, \quad (7)$$

$$\alpha_{\pi s} = \frac{1 - gh^2}{3gh^2} + \frac{1 - g}{1 + 2g}, \quad (8)$$

$$\alpha_{\pi c} = \frac{1 - gh^2}{2gh^2} + \frac{1 - g}{1 + g} \quad (9)$$

and g and h are density and sound speed contrasts

$$g = \frac{\rho_f}{\rho_w} \quad h = \frac{c_f}{c_w}, \quad (10)$$

where index f concerns fish body and w relates to water. Values of all parameters important in the model, both for fluid body and for gas in swimbladder, are reported in Table 2.

In the asymptotic domains the model (5) behaves as follows:

$$ka \rightarrow 0 \quad X \rightarrow 0 \quad \Leftrightarrow \quad \frac{X}{Y} \rightarrow 0 \quad \Leftrightarrow \quad \sigma_{bs} \rightarrow X \quad (5a)$$

$$ka \rightarrow \infty \quad X \rightarrow \infty \quad \Leftrightarrow \quad \frac{Y}{X} \rightarrow 0 \quad \Leftrightarrow \quad \sigma_{bs} \rightarrow YR^2 \quad (5b)$$

Table 2. Model parameters for fluid body and gas swimbladder.

	g	h	$\alpha_{\pi s}^2$	$\alpha_{\pi c}^2$	R^2	C_{sph}	C_{elli}	C_{bcyl}
fluid	1.043	1.052	0.0034	0.0077	0.0021	6.366	6.387	$3.593 \cdot H^2 L^2 / \rho_c a$
gas	0.00129	0.218	$2.96 \cdot 10^7$	$6.65 \cdot 10^7$	0.9989	$1.2 \cdot 10^8$	$1.2 \cdot 10^8$	$6.66 \cdot 10^7 \cdot H^2 L^2 / \rho_c a$

For all of these models, the long-wave region of scattering is determined by α and the geometrical region is controlled by the reflection coefficient R :

$$\begin{aligned} \sigma_{bs} &\sim \alpha^2 && \text{for } ka < 1, \\ \sigma_{bs} &\sim R^2 && \text{for } ka > 1. \end{aligned} \quad (11)$$

Shape elongation at constant volume makes the minor axis of ellipsoid or cylinder radius decreasing

$$a \propto (L/a)^{-1/3},$$

where L/a is major axis to semi-minor axis ratio (prolate spheroid) or length to radius ratio (cylinder). It is shown in Fig.1. On the other hand, in both cases, increasing L/a causes TS in asymptotic area ($ka \rightarrow \infty$) to increase:

for ellipsoid:
$$\sigma_{bs} = \frac{1}{16} L^2 R^2 \propto \left(\frac{L}{a}\right)^{4/3}, \quad (12)$$

for bent cylinder:
$$\sigma_{bs} = \frac{1}{4} \rho_c a R^2 \propto \left(\frac{L}{a}\right)^{1/3}. \quad (13)$$

Changing an L/a ratio from 10 to 40 results in the following rising of TS :

$$TS\left(\frac{L}{a} = 40\right) - TS\left(\frac{L}{a} = 10\right) = \begin{cases} 8 \text{ dB} & \text{for ellipsoid} \\ 2 \text{ dB} & \text{for bent cylinder} \end{cases}$$

This means that the effect of elongation will be stronger in the ellipsoid case. Fig.2 illustrates the dependence of target strength on frequency for all three model shapes, for the constant volume $V=100 \text{ cm}^3$ and for $L/a=20$. It was assumed $\rho_c/L=2$ for bent cylinder. There are almost no differences in the long-wave scattering region, but in the geometric region the elongated figures scatter more sound than the sphere of the same volume.

2. RELATIVE CONTRIBUTION OF DIFFERENT SIZE ORGANISMS TO THE TOTAL SOUND SCATTERING

The function

$$U(a, a_{\max}) = \frac{\int_{a_{\min}}^a N(a) \sigma_{bs}(a) da}{\int_{a_{\min}}^{a_{\max}} N(a) \sigma_{bs}(a) da} \quad (14)$$

allows us to evaluate the relative contribution of the objects with equivalent spherical radii less than a to the total scattering. In the case of power law size dependence of biomass (3) and the "high-pass" model of scattering (5), the volume backscattering coefficient takes the form:

$$S_v = \int N(a) \sigma_{bs}(a) da = \int B a^{-\kappa} \frac{D k^{-2} (ka)^6}{1 + C(ka)^4} da = BD k^{\kappa-3} \int \frac{(ka)^{6-\kappa}}{1 + C(ka)^4} d(ka) \quad (15)$$

where B , C and D do not depend on the integration variable ka . Quantities C and D depend on the shape and material of the object, and in the case of bent cylinder, on the degree of elongation L/a and curvature ρ_c/L (see Table 3).

Table 3. Expressions for C and D from formula (15) for different shapes.

	C	D
sphere	$\frac{4\alpha_{\pi s}^2}{R^2}$	$\alpha_{\pi s}^2$
ellipsoid	$\frac{16\alpha_{\pi c}^2}{9R^2}$	$\frac{1}{9}\alpha_{\pi c}^2 \left(\frac{L}{a}\right)^2$
bent cylinder	$\frac{\alpha_{\pi c}^2}{R^2} H^2 \frac{L^2}{\rho_c a}$	$\frac{1}{4}\alpha_{\pi c}^2 H^2 \left(\frac{L}{a}\right)^2$

For marine organisms without swimbladder the relative contribution to scattering can be described by the function:

$$U(a, a_{\max}) = \frac{\int_{x_{\min}}^x f(x) dx}{\int_{x_{\min}}^{x_{\max}} f(x) dx} \quad (16)$$

where $x_{\min} = ka_{\min}$, $x_{\max} = ka_{\max}$. The integral function

$$f(x) = \frac{x^{6-\kappa}}{1 + Cx^4} \quad (17)$$

is a function of variable ka and depends on the exponent κ and constant C . The result of integration obviously depends on the shape of integral function, which possess the maximum only for some types of the power distribution $N(a) \sim a^{-\kappa}$, namely for $2 < \kappa \leq 6$. For $\kappa = 6$, $f_{\max} = 1$ at $x_{\max} = 0$, for other cases we have:

$$f_{\max} = \frac{\left[\frac{6-\kappa}{C(\kappa-2)} \right]^{(6-\kappa)/4}}{1 + \frac{6-\kappa}{\kappa-2}} \quad (18a)$$

$$x_{\max} = \left[\frac{6-\kappa}{C(\kappa-2)} \right]^{1/4} \quad 2 < \kappa \leq 6 \quad (18b)$$

Fig.3 shows the function $f(x)$ for different values of coefficient κ and sphere model ($C=6.366$). Fig.4 presents the same function (17) for $\kappa = 4$ and different values of the quantity C . It can be seen that $f(x)$ (17) has the non-zero values for $ka < 1$ only. Fig.5 shows the dependence of x_{\max} and f_{\max} on C for three values of κ . Increasing C causes the maximum of the integral function to lower and to move towards smaller values of the argument. When κ increases, the maximum of the integral function moves towards zero and its value rises.

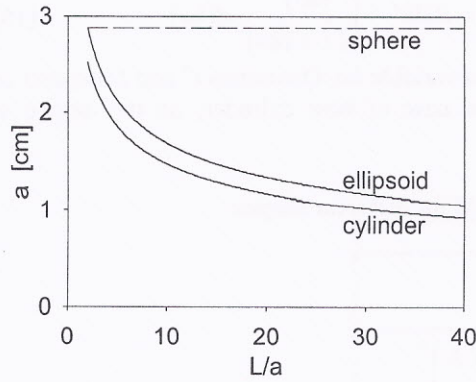


Fig.1. Dependence of scatterer radius on L/a ratio.

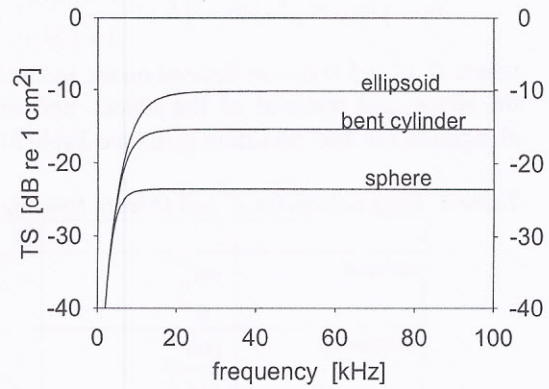


Fig.2. Target strength vs frequency for different scatterer shapes ($V=100 \text{ cm}^3$, $L/a=20$, $\rho_c/L=2$).

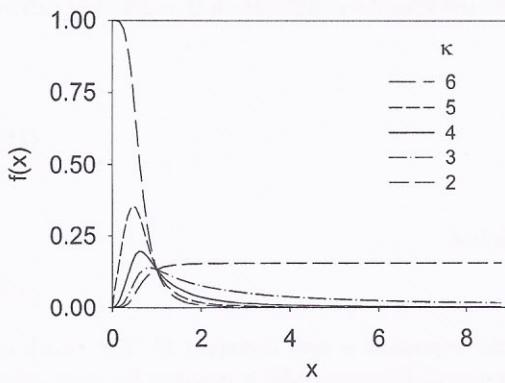


Fig.3. Integral function (17) for different κ values (sphere model).

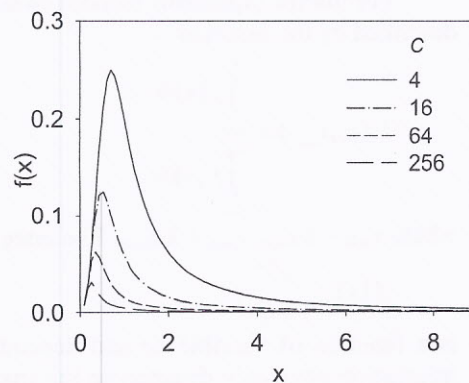


Fig.4. Integral function (17) for different C values ($\kappa = 4$).

For organisms equipped with swimbladder the scattering becomes important already in the long-wave region due to large elasticity of gas. Backscattering cross-section of fish with swimbladder is a sum of backscattering cross-section of the fluid body and of backscattering cross-section of the gas swimbladder:

$$\sigma_{bs} = \sigma_{bs,f} + \sigma_{bs, sb} \tag{19}$$

It is often assumed in fisheries acoustics that to ensure neutral buoyancy the swimbladder volume should stand for 5% of the total fish volume

$$V_{sb} = 0.05 V_f \tag{20}$$

If we assume that the swimbladder shape is similar to the whole organism shape, then the swimbladder radius or its semi-minor axis can be described as:

$$a_{sb} = \gamma a_f, \text{ where } \gamma = 20^{-1/3} \tag{21}$$

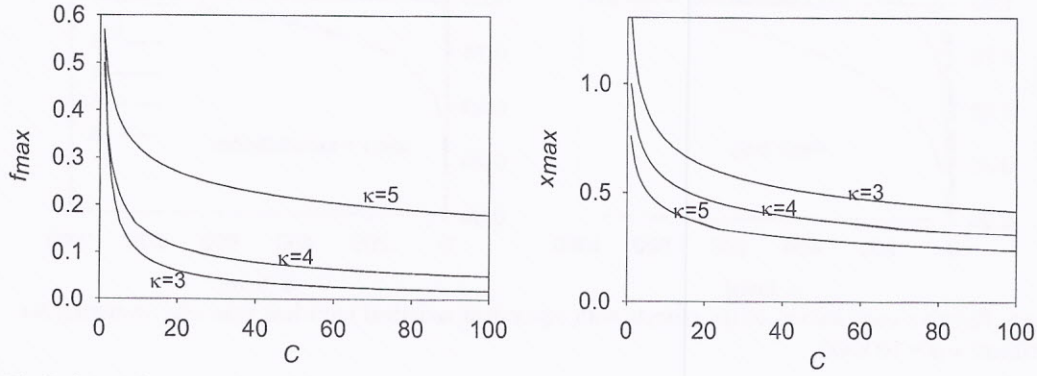


Fig.5. f_{max} and x_{max} vs C for different κ .

In such a case, the total backscattering cross-section of the unit volume can be expressed as follows:

$$\int N(a) \sigma_{bs}(a) da = BD_f k^{\kappa-3} \int \frac{(ka)^{6-\kappa}}{1+C_f(ka)^4} d(ka) + BD_{sb} \gamma^6 k^{\kappa-3} \int \frac{(ka)^{6-\kappa}}{1+\gamma^4 C_{sb}(ka)^4} d(ka) \quad (22)$$

So, in the case of swimbladder fish, the relative contribution to scattering takes more complicated form as compared to (15):

$$U(a, a_{max}) = \frac{D_f \int_{a_{min}}^a \frac{x^{6-\kappa}}{1+C_f x^4} dx + \gamma^6 D_{sb} \int_{a_{min}}^a \frac{x^{6-\kappa}}{1+C_{sb} x^4} dx}{D_f \int_{a_{min}}^{a_{max}} \frac{x^{6-\kappa}}{1+C_f x^4} dx + \gamma^6 D_{sb} \int_{a_{min}}^{a_{max}} \frac{x^{6-\kappa}}{1+C_{sb} x^4} dx} \quad (23)$$

Both terms of the above expression have maxima located in different areas – swimbladder at $ka < 0.05$ and flesh at ka close to 1, and what is important, there are 5 orders of difference in the height of these maxima.

The calculations of $U(a, a_{max})$ were carried out from $a_{min}=0.1$ mm to $a_{max}=1$ m, frequency $f=1, 10$ and 100 kHz, three shapes of scatterers, $\kappa=3, 4, 5, 6$. Fig.6 is an example of such calculations for the prolate spheroid. It presents $U(a, a_{max})$ for the frequency 10 kHz and for four values of κ . The left part concerns fish body only, the right one – body and swimbladder. It allows estimating the size of scatterer at which some fixed percent of total scattering takes place. If we consider, for example, $\kappa=4$, then we can state that organisms with equivalent spherical radius $a_{e, sph}$ smaller than 120 mm are responsible for 90% of scattering in the no-swimbladder case and that organisms with equivalent spherical radius $a_{e, sph}$ smaller than 6 mm scatter 90% of the entire acoustic energy in the swimbladder case. The bigger κ is, the stronger is that effect. The frequency is also substantial, because it determines the ka -threshold between long wave and short wave scattering regions characterised by weak and strong scattering, respectively. Such calculations make sense only for the cases near to “saturation”, when the integral function is tending asymptotically to zero (for $\kappa > 3$ only). In the other cases, the objects bigger than a_{max} , from beyond the integration interval, give the relevant contribution to scattering. The results of calculations for two other shapes of scatterers (sphere and bent cylinder) and for different degree of elongation are almost the same as presented for ellipsoid in Fig.6.

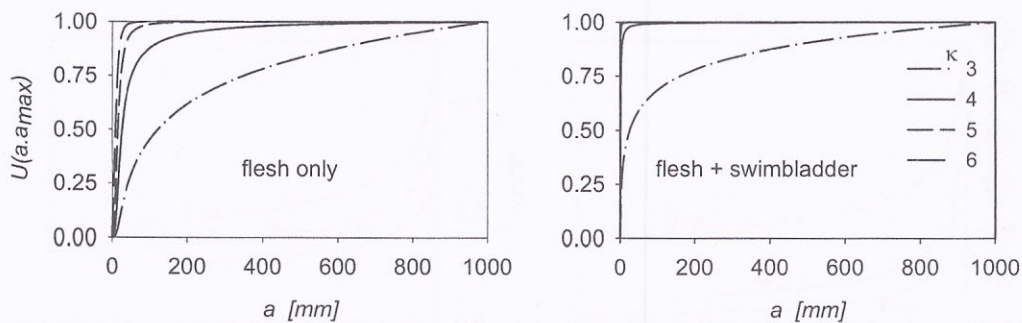


Fig.6. Relative contribution of the objects with equivalent spherical radii less than a to scattering for different κ ($f = 10$ kHz).

So far, our consideration did not concern the resonance of the swimbladder, which is crucial in the case of scattering on fish. The resonance is connected with very strong vibrations of gas in the region of $ka \approx 0.01$. If we assume that the smallest fish with a swimbladder has $a_{e,sph} = 2$ mm, then the radius of its swimbladder is ~ 0.8 mm. This gives the resonance frequency approximately 4-5 kHz. All the bigger fish will possess bigger swimbladders resonating below 4 kHz. Therefore, the majority of frequencies used in fisheries acoustics are located below the resonance peak, but still on its declining slope.

3. DISCUSSION

It has been shown that for statistical distribution of the marine biomass of the form $N(a) = Ba^{-\kappa}$ and for the "high-pass" model of scattering, the relative contribution to scattering reaches the maximum value 1 for different values of scatterer size, which depends on the character of the size spectrum and the frequency of sound. The higher frequency and the higher value of κ is, the smaller is this critical size above which there is no relevant scattering.

REFERENCES

1. D.Chu, Z.Ye, A phase-compensated distorted wave Born approximation representation of the bistatic scattering by weakly scattering objects: Application to zooplankton, *J.Acoust.Soc.Am.*, 106, 4, Pt.1, 1732-1743, 1999.
2. Gorska. N., Chu D., Some aspects of sound extinction by zooplankton. *J.Acoust.Soc.Am.*, 110, 2315 – 2325, 2001.
3. P.Greenblatt, Sources of acoustic backscattering at 87.5 kHz, *JASA*, 70(1), 134-142, 1981.
4. C.Javanaud, The effect of the choice of formula for target strength on the evaluation of the volume backscattering strength, *Acoust.Lett.*, 14(6), 101-109, 1990.
5. R.K.Johnson, Sound scattering from a fluid sphere revisited, *JASA*, 61(2), 375-377, 1977.
6. R.W.Sheldon, A.Prakash, W.H.Sutcliffe, Jr., The size distribution of particles in the ocean, *Limn.Oceanogr.*, 17(3), 327-340, 1972.
7. T.K.Stanton, Simple approximate formulas for backscattering of sound by spherical and elongated objects, *JASA*, 86(4), 1499-1510, 1989.
8. T.K Stanton, D.Chu, D., P.H. Wiebe, Acoustic scattering characteristics of several zooplankton groups. *ICES Journal of Marine Science*, 53, 289-295, 1996.